Development of a DSO Support Tool for Congestion Forecast

Received: 28 May 2021 | Revised: 19 July 2021 | Accepted: 3 August 2021

IET Generation, Transmission & Distribution

DOI: 10.1049/gtd2.12266

The Institution of Engineering and Technology WILEY

ORIGINAL RESEARCH PAPER

Development of a DSO support tool for congestion forecast

Ankur Srivastava[1] | **David Steen**[1] | **Le Anh Tuan**[1] | **Ola Carlson**[1] | **Ioannis Bouloumpasis**[1] | **Quoc-Tuan Tran**[2] | **Lucile Lemius**[3]

[1] Division of Electric Power Engineering, Department of Electrical Engineering, Chalmers University of Technology, Gothenburg, Sweden

[2] Department of Solar Technologies, Université Grenoble Alpes, CEA, LITEN, INES, Le Bourget du Lac, France

[3] Department of Smart Utilities, Atos Worldgrid, Grenoble, France

Correspondence
Ankur Srivastava, Division of Electric Power Engineering, Department of Electrical Engineering, Chalmers University of Technology, Gothenburg, Sweden.
Email: ankur.srivastava@chalmers.se

Funding information
European Commission, Grant/Award Numbers: 773717, 864048

Abstract

This paper presents a novel DSO support tool with visualisation capability for forecasting network congestion in distribution systems with a high level of renewables. To incorporate the uncertainties in the distribution systems, the probabilistic power flow framework has been utilised. An advanced photovoltaic production forecast based on sky images and a load forecast using an artificial neural network is used as the input to the tool. In addition, advanced load models and operating modes of photovoltaic inverters have been incorporated into the tool. The tool has been applied in case studies to perform congestion forecasts for two real distribution systems to validate its usability and scalability. The results from case studies demonstrated that the tool performs satisfactorily for both small and large networks and is able to visualise the cumulative probabilities of nodes voltage deviation and network components (branches and transformers) congestion for a variety of forecast horizons as desired by the DSO. The results have also shown that explicit inclusion of load-voltage dependency models would improve the accuracy of the congestion forecast. For demonstrating the applicability of the tool, it has been integrated into an existing distribution management system via the IoT platform of a DMS vendor, Atos Worldgrid.

1 | INTRODUCTION

1.1 | Motivation

Global warming concern leads the transition from fossil fuels to renewable energy sources (RES) for the generation of electricity. The European Green Deal envisions Europe to be climate-neutral by 2050 through maximising the deployment of renewables and fully decarbonising the energy supply [1]. The International Renewable Energy Agency (IRENA) and European Commission in their REmap analysis in ref. [2] have identified that the European Union has the potential to generate 50% of the total electricity generation from renewables by 2030. Under this scenario, wind power would account for 21% (783 TWh) and solar photovoltaics (PV) for 8% (281 TWh) of the total generation. Similar trends for increasing renewables share could be seen for other countries as well.

Across the globe, multiple incidents related to network congestion are reported in refs. [3–5] due to the higher penetration of RES. A study on congestion events in the distribution systems caused due to RES in Germany is presented in ref. [6]. The study further presents that due to increasing RES penetration the total amount of energy curtailment in 2014 was the same as the aggregated amount from 2009 to 2013 and it is growing further. It mentions that the German Federal Network Agency reported that the majority of this curtailment (92.2%) was on the distribution grid side as most of the RES is connected here. The work presented in ref. [7] shows how the battery energy storage systems (BESS) could aggravate the network congestion issues. It occurs when BESS starts charging as soon as the surplus power (after self-consumption) is available, leading to full-charge before the peak PV production occurs in the day. Thus, during the peak PV production, the power is being fed into the grid and which causes network congestion.

Due to the anticipated increased penetration of RES in distribution systems and more uncertain loads such as heat pumps, electric vehicles etc., the distribution system operators (DSOs) are expected to face increasing component congestion and voltage variation issues in their networks [8]. In addition to such operational problems, the DSOs are also likely to face issues

such as loss of life of the network components (transformers, distribution lines, and cables), the need for grid reinforcement and/or flexibility services, RES generation curtailments due to network constraints, generation scheduling [9, 10] etc. A study presented in ref. [11] has estimated that Sweden, Germany, and the UK with their current grid capacity can supply 24%, 60%, and 21% respectively, of the annual net electricity consumption from residential solar PV. Thus, if the PV generation exceeds the anticipated amount then it could lead to operational challenges like network congestion etc., as mentioned before.

There has been extensive ongoing research for congestion management in distribution systems. For instance, in ref. [12], a real-time congestion management method based on the flexibility services from electric vehicles and heat pumps is proposed. The method expects that the DSO has the ability to forecast network congestion. The need for such forecasts is also emphasised in ref. [13], which mentions that with regard to market-based congestion management models relying on flexibility, forecasting the volume of congestion would require load forecasting and state estimation of the distribution system. In ref. [14], a distributed optimisation-based dynamic tariff method is proposed for congestion management, which requires the inputs of the congestion forecast, but the method and the characteristics of such a congestion forecast are not presented in detail. Similarly, a multi-objective congestion management approach is proposed in ref. [15] which utilises the generation rescheduling and load shedding along with the inclusion of voltage-dependent load models.

Most of these works have either mentioned the need for the congestion forecast or have simply assumed that the DSOs have the capability to forecast the congestion. From these discussions, it is evident that there is an emerging interest in a solution for a fast and accurate congestion forecast which can forecast congestion in different time horizons. An accurate congestion forecast would allow the DSOs to efficiently manage the network congestion by employing their desired congestion management methods.

A few research works have addressed the congestion forecast issue, e.g. ref. [16], in which a probabilistic method is developed for detecting and ranking the congested lines to help network operators. A congestion forecast framework is proposed in ref. [17], which considers only snapshot data of system uncertainties with limited visualisation of network congestion. However, what is expected to be primarily needed by the DSOs in the coming years is a compact tool that can forecast network congestion on different timescales and has interactive visualisation capabilities. Further, the inclusion of other operating conditions such as PV-inverter operating modes and load models within such congestion forecast tool would be an enhancement for the DSOs.

The probabilistic approach is widely accepted for modelling uncertainties. Several research works have used this approach for different applications. As in ref. [18], a probabilistic algorithm is developed to evaluate the capacity of power reserve for a system with high PV penetration. The authors in ref. [19] used it for the evaluation of the maximum integration limits for distributed generations with voltage constraints. A simplified version of the backward-forward sweep (BFS) method, which employs a Gaussian mixture distribution, is proposed to solve probabilistic power flow (PPF) more efficiently to be used for the planning of LV networks in ref. [20]. Similarly, a new probabilistic method is proposed in ref. [21], which is based on quasi-static time-series analysis in combination with the golden section search algorithm to prevent reverse power flow in distribution systems due to PV integration. The impact of uncertainty associated with distributed energy resources (DERs) is analysed in ref. [22], and the benefits of installing microgrids to address such challenges are also demonstrated. Thus, the probabilistic approach is utilised for addressing several research problems in the distribution systems; however, most of the existing works have not addressed the research problem associated with the forecasting of network congestion.

While, on the commercial side, among the available solution's for the advanced distribution management system (ADMS) such as Network Manager by Hitachi ABB [23], Spectrum Power by Siemens [24], EcoStruxure by Schneider Electric [25] etc., provide functionalities such as DERs production forecast, demand forecast, state estimation, load flow, protection etc. In general, most of the ADMS solutions have several advanced functionalities which are associated with the evolution of distribution systems. However, the congestion forecasting functionality is not explicitly included or addressed in these ADMS solutions.

1.2 | Contributions

Today, the DSOs are not equipped with similar congestion forecast tools, at least at an operational level. However, some DSOs may have already invested in research approaches to develop similar tools, driven by the expected increased congestion incidents. Thus, keeping in mind today's and future need of the DSO related to the accurate forecast of congestion levels in their network, a novel congestion forecast tool has been developed and demonstrated in this paper.

The main contributions of the paper can be summarised as follows:

- Development of a congestion forecast framework using probabilistic power flow incorporating advanced PV production and load forecasts.
- Incorporation of the load-voltage dependency models in congestion forecast framework for enhanced accuracy of power flow solution and probable operating modes of PV inverters for a realistic reactive power support capability from PV inverters.
- Development of customised visualisation functionality in the ADMS for presenting the congestion forecast results to the DSO.
- Integration of the developed congestion forecast tool to the existing distribution management system (DMS) via an IoT platform Codex Smart Edge of a DMS vendor, Atos Worldgrid.

- Demonstration of the use of the tool using real network data as well as in the real environment with system integration of Atos DMS's to the real demonstration site of SOREA, a small French DSO.

The rest of the paper is organised as follows; Section 2 describes the functionalities of the congestion forecast tool. The modelling of the different components in the tool is presented in Section 3. Section 4 presents the details of the case studies, while the results and discussions are presented in Section 5. The scalability and accuracy of the tool are discussed in Section 6. The details of the tool integration and demonstration are presented in Section 7. The concluding remarks are outlined in Section 8.

2 | CONGESTION FORECAST TOOL DESCRIPTION

This section presents an overall description and features of the proposed congestion forecast tool including the inputs, visualisation of forecast results and discusses the possible applications of the tool from the DSO's perspective. The modelling of the probabilistic power flow framework and other associated elements are discussed in Section 3.

2.1 | Inputs

The various inputs required for the congestion forecast tool are as follows:

2.1.1 | System data

It includes the network parameters, branches ampacity, and transformers rated capacity. It can be provided in different data formats as separate input files by the DSO. For the integration of the tool with the DMS of the DSO, it can be provided through existing SCADA/DMS. Also, the updated network configuration is provided by the DSO in real-time as an input to the tool. In case of network reconfiguration, the tool needs to be re-run with the new network topology over all the forecast horizons because as the network configuration changes, the power flow results would change which will have an impact on the congestion forecast results.

2.1.2 | Forecast of PV production and load

It includes the forecasts of PV production and load, load model parameters. The forecasts errors are also inputs to the tool and should be made available to the DSO through the PV production and load forecasts services.

2.1.3 | DSO preferences

It includes the number of Monte-Carlo simulations (MCS), node voltage limits, PV-inverter operating mode, and tolerance limits.

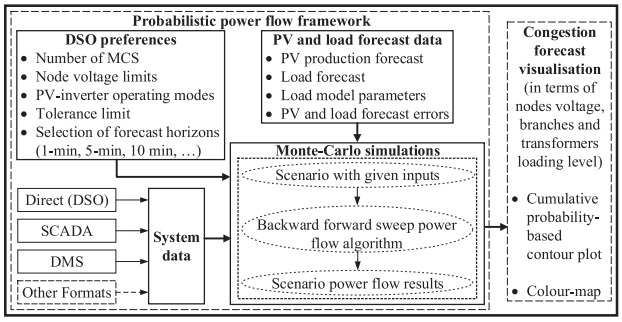

FIGURE 1 Flow chart of the congestion forecast tool

These preferences are set as a default value but can be altered by the DSO.

The flow chart of the congestion forecast tool along with the preferences is presented in Figure 1.

2.2 | Visualisation of congestion forecast results

The congestion forecast visualisation helps the DSO in identifying the exact location and severity of congestion and assists them in taking suitable mitigating actions such as market participation, flexibility procurement etc. The main features of the congestion forecast visualisation are:

2.2.1 | Congestion forecast indicators

The following indicators are proposed for congestion forecast visualisation:

- Cumulative probability-based contour plot: Cumulative probability (CP) denotes the probability of a variable reaching a level equal to or greater than a threshold. Here, the CPs are calculated with the desired threshold for all the chosen congestion indicators such as nodes voltage and components overloading. They are used for contour plots, which help the DSO in understanding the congestion severity in a specific node and component.
- Colour-map: Colour-map (CM) is the colour-based representation of the network, indicating the severity and the exact location of the congestion.

2.2.2 | Congestion forecast horizons selection

With the proposed congestion forecast tool, network congestion forecast can be made with various forecasting horizons depending on the needs and operation strategies of the DSO on how they tackle the possible congestion in their network in different time-frames. The details of the possible forecast horizons, along with the selection reasoning, are presented in Table 1. For instance, 5-min ahead forecast horizon value is selected by

TABLE 1 Congestion forecast horizons with selection reasoning

Sl. no.	Forecast horizons	Reason for selection	Forecast value selection
1	1-min ahead	Evaluate real-time congestion status	Next minute (0th–1st) forecasted value
2	5, 10, and 15-min ahead	Identify congestion forecast in close to real-time conditions	Average of the forecasted values for 0th–5th, 5th–10th, and 10th–15th min
3	30, 45, and 60-min ahead	Set up a close to real-time congestion management plan	Average of the forecasted values for 15th–30th, 30th–45th, and 45th–60th min
4	2, 3, ⋯ 24-hour ahead	Set up an intra-day congestion management plan	Peak value among the average of forecasted values for four 15-min time slots between 1st–2nd, 2nd–3rd, ⋯ and 23rd–24th hour

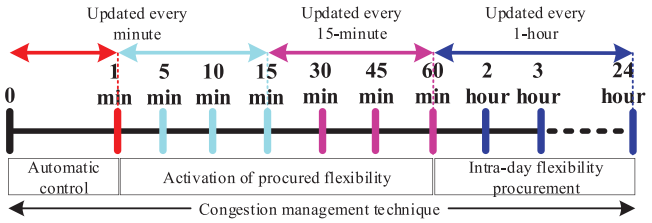

FIGURE 2 Strategic selection of forecast horizons along with the respective congestion management strategies

taking the average of five forecast values between the 0th and 5th min. It should be noted that these time-horizons can be customised by the DSO. The possible congestion management strategies with various time-horizons which can be taken by the DSO are shown in Figure 2.

2.3 | Real application from industry perspective

The congestion forecast tool will assist the DSO in the daily congestion management and network planning, depending on the forecast horizons. In short forecast horizons, the DSO will be enabled with timely congestion management by employing market and tariff-based flexibility solutions [26]. It would result in enhancement of the system's resilience, mitigation of equipment ageing due to overloading, reducing the high additional congestion cost, and other economic benefits. While, long-term forecast horizons (e.g. several months or years ahead) will allow the DSO to procure flexibility for avoiding costly grid reinforcement. The visualisation platform provided by the tool will facilitate the effective supervision of the desired network operation via an on-time and user-friendly indication of the expected network congestions. Therefore, the implementation of the developed tool will result in reduced cost for grid reinforcement and purchasing flexibility resources for the DSOs. The integration of the congestion forecast tool in the commercial ADMS solutions would provide them a competing edge over other existing ADMS solutions. This paper explores the possibility for commercialisation of the developed tool through integration with the Codex Smart Edge solution of Atos Worldgrid.

FIGURE 3 Fisheye lens camera and its installation at Sorea's site in France

3 | MODELLING

This section presents the modelling approach associated with the different components in the congestion forecast tool.

3.1 | PV production and load forecasts modelling

This subsection presents the details of the forecast techniques used for PV production and load forecasts. Due to increasing PV penetration and intermittent loads in the distribution systems, their modelling is an important aspect of the congestion forecast tool. The modelling employs different methods for the PV production and load forecasts. Also, the time-horizon of the two forecasts are different. The PV production forecast is done with a very short time horizon, i.e. a minute ahead, by employing machine learning techniques that use sky-images and fine modelling of the cloud cover motion and the built-in combination with the on-site all-sky imager, while the load forecast is done in relatively long time horizon, i.e. 1 hour, through an artificial neural network model.

3.1.1 | PV production forecast

A near-real-time (1 min-ahead) PV production forecast solution is used in this work. The choice of the acquisition system is focused on a camera equipped with a fisheye lens whose viewing angle is 180° (horizon to horizon coverage). Figure 3 shows the fisheye camera used for the acquisition and its installation at Sorea's site in France [27].

This acquisition system works on the principle of observing the cloud cover by taking periodic images of the sky, followed by processing these images, and then integrate the PV forecast into the forecast tool. This system generates a new forecast every

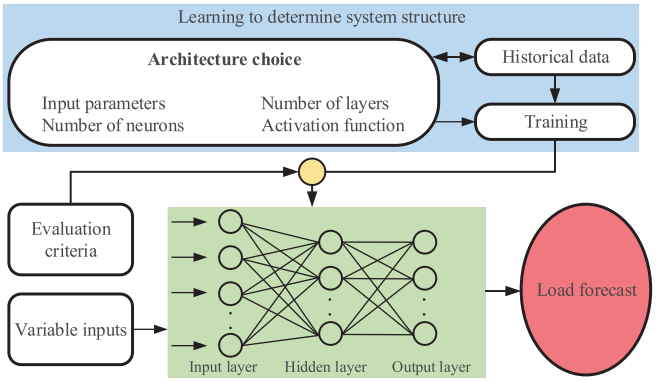

FIGURE 4 Functional diagram for ANN-based load forecast method

minute with a resolution of 1 min until the 24th hour of the concerned day. The description of the different steps involved in the algorithm used for the PV production forecast is as follows:

Step 1. Pre-treatment: The sky images captured by the camera are not fully adapted to this application and hence require treatment before being processed. The resolution of the captured images plays an important role in the forecast. Interestingly, the low-resolution images do not have a significant impact on the output, as cloud movements (and their deformations) are not perfectly predictable. Thus, one of the pre-treatment includes reducing the resolution of the captured images.

Step 2. Cloud detection and motion estimation: The next step is the processing of sky images to perform the area segmentation for cloud detection and motion (speed) estimation. Sometimes, the algorithm could also select the unwanted reflections and thus performs post-treatment to eliminate them.

Step 3. Cloudy weather forecast: After estimating the segmented clouds and their displacements, the prediction of their future displacement could be easily done. This step helps in understanding the future path of clouds and how the clouds will cover the sun over the next minutes.

Step 4. Forecast of PV production: The clouds movement prediction information along with the PV plant characteristics is used for forecasting the amount of radiation received and hence the forecast of PV power production.

3.1.2 | Load forecast

An artificial neural network (ANN) based short-term (1 hour-ahead) load forecasting is used in this work. The model is implemented using the Neural Networks Toolbox in MATLAB. The functional diagram for the ANN-based load forecast method is shown in Figure 4. Multiple tests cases are realised to obtain the best ANN architecture in terms of the number of hidden layers and number of neurons in each layer. A feed-forward model and back-propagation learning algorithm are used for the ANN model and weights adjustment. The transfer functions used are the step and sigmoid. The load forecasting model takes into account the different inputs categories such as weather, calendar, and load, which are presented in Table 2. The load forecast is generated every hour with a resolution of 1 hour until the 24th hour of the concerned day. Since the load forecast technique has an hourly resolution, the load forecast values for horizons less than an hour are taken as forecast values for that hour.

TABLE 2 Input data for the ANN-based algorithm

Category	Variable	Type
Weather	Temperature	Actual value
Calendar	Hour of day	Actual value (0-23)
	Day of week	Monday = 0, Tuesday = 1, ... , Sunday = 6
	Type of day	Non-working day = 0, working day = 1
	Month	January = 0, February = 1, ... December = 11
Load	Growth rate	Actual value
	Power	Actual value

It should be noted that the load forecast implicitly considers the charging and discharging of energy storage. The load forecast is based on the measurement data of aggregated loads which include energy storage devices. Thus, the charging and discharging of energy storage will not have a direct impact on the load forecast results presented in this paper. However, the explicit inclusion of charging and discharging of energy storage as the input signal in the load forecast would further enhance the accuracy of the results.

3.2 | Load modelling

This subsection presents the details of the inclusion of load models into the tool. Usually, the constant power load model is considered where the loads are assumed to remain independent of the system voltage. The active and reactive load characteristics for a combination of constant power (P), constant current (I), and constant impedance (Z), called as *ZIP* load model, can be expressed as a function of voltage [28]:

$$P = P_0 \left[k_{P_p} + k_{P_I} \left(\frac{V}{V_0} \right) + k_{P_Z} \left(\frac{V}{V_0} \right)^2 \right] \quad (1)$$

$$Q = Q_0 \left[k_{Q_p} + k_{Q_I} \left(\frac{V}{V_0} \right) + k_{Q_Z} \left(\frac{V}{V_0} \right)^2 \right] \quad (2)$$

where V_0 represents the nominal voltage, k_{P_p} and k_{Q_P} are constants representing the proportion of P load, k_{P_I} and k_{Q_I} are constants representing the proportion of I load, k_{P_Z} and k_{Q_Z} are constants representing the proportion of Z load, for active and reactive power load, respectively. The different load model parameters are considered in this work and presented in Table 3.

TABLE 3 Load model parameters for different cases

Sl. no.	Load type	Active power coefficients			Reactive power coefficients		
		k_{P_P}	k_{P_i}	k_{P_z}	k_{Q_P}	k_{Q_i}	k_{Q_z}
1	Constant power	1	0	0	1	0	0
2	Residential feeder	0.10	0.85	0.05	0.00	0.65	0.35
3	Constant impedance	0	0	1	0	0	1
4	Equal proportion of ZIP load	0.33	0.33	0.33	0.33	0.33	0.33

The following steps are iterated to include the load models in the probabilistic power flow calculation [29]:

Step 1: Initial values of voltage at all the system nodes are taken as one p.u.
Step 2: Calculate load values with the inclusion of load models.
Step 3: Calculate branch currents and new node voltages.
Step 4: Update the values of both active and reactive loads with new node voltages.

3.3 | Operating modes of PV-inverter

Due to increased DERs penetration, there are stricter requirements in new standards for DERs interconnection with the distribution grid when compared to previous ones. Some of these interconnection requirements are mentioned in the recent IEEE standard on the interconnection and interoperability of DERs [30]. The two most common operating modes of PV-inverter are constant power factor and voltage-reactive power. In this paper, it is assumed that PV-inverter operates in both modes. These modes are incorporated into the tool to mimic the interconnection requirements as follows:

3.3.1 | Constant power factor mode (constant-pf)

In this mode, all the nodes except the slack node are modelled as *P*-*Q* nodes. The PV production at all the nodes is modelled as a negative load and with a constant power factor. The step-wise formulation of the BFS algorithm in this mode for the pth iteration, are as follows:

Step 1: A flat voltage profile is taken for all nodes except the slack node, which is kept constant.
Step 2: Calculate current injection at node r, as:

$$A_r^{(p)} = \left[\frac{S_r}{V_r^{(p-1)}}\right]^* - Y_r V_r^{(p-1)} \quad \forall\, r = 1, 2, \ldots, N \tag{3}$$

Step 3: Calculate branch currents (in branch q) in the backward direction starting from the last node, as:

$$I_q^{(p)} = A_n^{(p)} + \sum_{b=1}^{t} I_b^{(p)} \quad \forall\, q = br, \ldots, 2, 1 \tag{4}$$

Step 4: Update node voltages (at node n) in the forward direction starting from the slack node, as:

$$V_n^{(p)} = V_m^{(p)} - Z_q I_q^{(p)} \quad \forall q = 1, 2, \ldots, br \tag{5}$$

where N, br, t, and Z_q represent the total number of nodes, total number of branches, total number of branches connected at node n, and the impedance of branch q, respectively.

These steps are iterated until the convergence criterion is reached.

3.3.2 | Voltage-reactive power mode (constant-V)

In this mode, the PV production nodes are modelled as *P*-*V* nodes and load nodes are modelled as *P*-*Q* nodes. A compensation method is used for the elimination of voltage mismatches from their specified values at *P*-*V* nodes [31]. The step-wise formulation of voltage mismatch compensation in addition to the BFS algorithm for k *P*-*V* nodes in the system and pth iteration are as follows:

Step 1: Calculate voltage magnitude mismatch at rth node, as:

$$\Delta V_r^{(p)} = \left|V_r^{(s)}\right| - \left|V_r^{(p)}\right| \quad \forall\, r = 1, 2, \ldots, k \tag{6}$$

Step 2: Calculate the reactive current injection at rth node, as:

$$I_{rQ}^{(p)} = j\left|Z_r^{-1}\Delta V_r^{(p)}\right| \quad \forall\, r = 1, 2, \ldots, k \tag{7}$$

Step 3: Calculate the total reactive power requirement Q_{rR} at rth node, as:

$$Q_{rR}^{(p)} = Q_r^{(p)} + Q_{rL}$$
$$Q_r^{(p)} = \mathrm{Im}[V_r I_{rQ}^{\prime\,*}{}^{(p)}] \quad \forall\, r = 1, 2, \ldots, k \tag{8}$$

Step 4: Check whether the calculated Q_{rR} (=Q_{inj}) satisfies:

$$P_{\mathrm{inj}}{}^2 + Q_{\mathrm{inj}}{}^2 \le S_{\mathrm{rated}}{}^2 \quad \forall\, r = 1, 2, \ldots, k \tag{9}$$

Otherwise, calculate the new value of P_{inj} and Q_{inj} [17].

where $V_r^{(s)}$, Z, Q_{kL}, and I'_{kQ} represents the specified voltage value at node r, a real and constant impedance matrix, reactive power load at node k, and the sum of the required reactive current and load current injection.

These steps are iterated until the voltage mismatches for all P-V nodes reach within the tolerance limit.

3.4 | Probabilistic power flow method

The probabilistic approach is used to model the uncertainties in the proposed congestion forecast tool. MCS is employed to run a large number of scenarios to incorporate PV production and load forecasts in the system. BFS method is used for solving the power flow algorithm. This work considers the Gaussian probability density function (PDF) which is a commonly used for generating MCS values using the values obtained from PV production and load forecasts [22], as described by Equation (10):

$$\text{PDF} = \frac{1}{\sqrt{2\pi\sigma^2}} e^{-\frac{(x-\mu)^2}{2\sigma^2}} \tag{10}$$

where mean (μ) is the value of PV production and load forecasts, while standard deviation (σ) depends on forecast type and horizon.

3.5 | Results of congestion forecast

The congestion results are extracted from the power flow results of MCS presented in Section 3.4. To visualise the congestion forecast results, the following indicators are chosen:

- Node voltage: It refers to the node voltage and deviation from its nominal value.
- Branch loading: It refers to the loading of a branch relative to its rated ampacity.
- Transformer loading: It refers to the loading of a transformer relative to its rated capacity.

4 | CASE STUDIES DESCRIPTION

4.1 | 7-bus feeder of Sorea's distribution system in France

The considered system, as shown in Figure 5, has a radial structure with seven nodes, including both medium- and low-voltage (MV and LV) nodes, five branches, and one MV-LV transformer (20/0.4 kV). The ampacity of all branches is assumed to be 350 A, while the rated capacity of the transformer is 250 kVA. Presently, the system has two PV installations at nodes 5 and 7 with the maximum capacity of 74 and 82 kWp (kilowatt peak), respectively. A camera-based acquisition system is installed at node 6 to be used for the PV production forecast. The network parameters are provided by the UNITED-GRID [32] project partner Sorea and presented in Appendix.

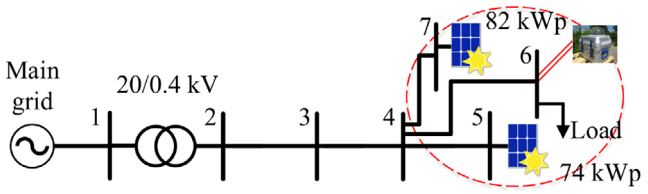

FIGURE 5 Single-line diagram of a part of Sorea's distribution system

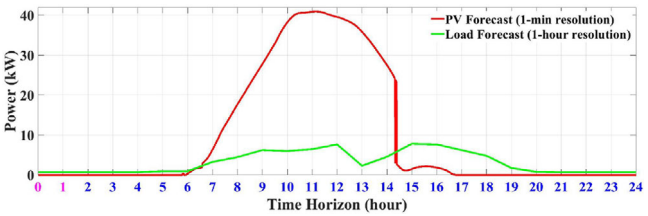

FIGURE 6 The PV production and load forecasts profile at 00:00 hour on 11th October 2018 over the next 24-hours for Sorea's site in France

The PV production and load forecasts data used in this case study are for 11th October 2018, as shown in Figure 6. The data shows that the PV production is forecasted to vary between 0 to 40.91 kW, while the load is forecasted to vary between 0 to 7.8 kW.

4.2 | 141-bus distribution system of Caracas metropolitan area

The considered system is a real distribution system in the metropolitan area of Caracas [33]. The system has a nominal voltage of 12.47 kV with 140 branches and 84 load buses. The system has been modified to include PV installations at all the load buses. The same PV production profile (without affecting the generality of the results), as shown in Figure 6, is considered at all the PV nodes. For a realistic load scenario, the feeders in the considered system are randomly divided into residential, commercial, and industrial areas. Further, the hourly load profiles at different nodes for these areas are presented in Figure 7, which are obtained from the real load data of a local DSO in Sweden. The single-line diagram for the 141-bus distribution

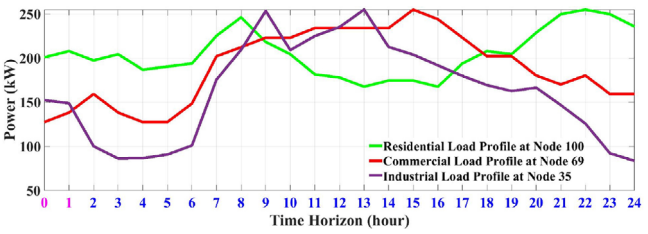

FIGURE 7 Residential, commercial, and industrial load profiles used in the 141-bus distribution system

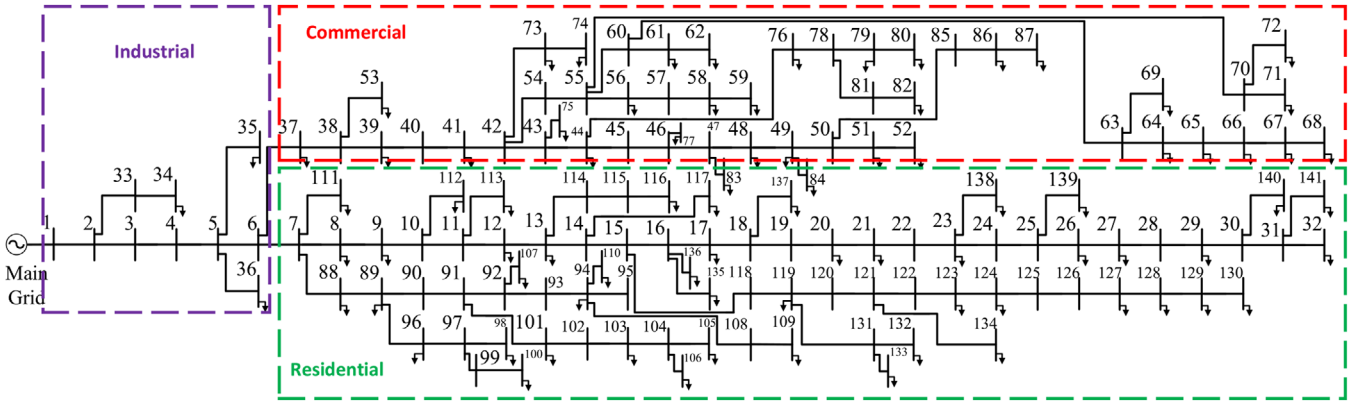

FIGURE 8 Single-line diagram of the 141-bus real distribution system in the metropolitan area of Caracas with PV installations

TABLE 4 PV production and load forecasts errors over different forecast horizons (in %)

Forecast error	Forecast type	Forecast horizons				
		1-min ahead	5, 10, and 15-min ahead	30, 45, and 60-min ahead	2, 3, ... 6-hour ahead	7, 8,... 24-hour ahead
Case 1	PV	1.0	3.0	5.0	8.0	10.0
	Load	5.0	5.0	5.0	5.0	8.0
Case 2	PV	1.5	4.0	6.0	9.0	12.0
	Load	6.0	6.0	6.0	6.0	10.0

system is shown in Figure 8. The branches' ampacity is assumed to be 1500 A.

To analyse the impact of load models on the congestion forecast accuracy, different cases are studied, which are presented in Table 3. These cases include constant P load, constant Z load, an equal proportion of ZIP load, and load model for a typical residential feeder. The coefficients of the load model for a residential feeder have been obtained using the real measurement data provided by a DSO in Sweden. The data include time-series measurement of active power (P), reactive power (Q), and voltage (V) from customers connected to a residential feeder [34]. From the data, the coefficients for the load model are obtained through a standard linear regression using least squares fit techniques. Subsequently, P and Q are represented as a function of voltage V using a polynomial model structure, as given by Equations (1) and (2).

As explained in Section 2.2.2, the congestion forecast is performed continuously on a rolling horizon. The PV production and load forecasts errors depend on the forecast horizon, and hence different errors are considered, as shown in Table 4. The PV production and forecast errors are considered as zero during the evening and night hours.

The proposed congestion forecast tool has been implemented using MATLAB R2019b and Python. The number of MCS is considered 10 000 [22], and the power flow convergence criterion is taken as 0.00001 p.u.

5 | RESULTS AND DISCUSSIONS

5.1 | 7-bus feeder of Sorea's distribution system in France

The visualisation of the congestion forecast over a day is presented through both CP-based contour plot and colour-map. The simulation is done with PV production and load forecasts data for 00:00 hour of 11th October 2018 under a constant-pf mode of PV-inverter.

5.1.1 | Cumulative probability-based contour plot

To illustrate the results of the congestion forecast, the CP for the voltage at node 5 is shown in Figure 9. The contour plot shows the difference over various forecast horizons. The CP for node voltage deviation remains low (green area) from 1-min to 7-hour ahead and then starts increasing (towards yellow area) until 13-hour ahead and subsequently starts decreasing. For the 13-hour ahead, the CP for node voltage to be above 1.04 p.u. is 0.7 (or 70% of the times). The colour bar in the contour plot represents the severity of congestion.

It is evident from Figure 9 that the network is subjected to different congestion levels over the considered forecast horizons. These changes in the congestion levels occur mainly due to varying PV production and load demand during the day. This

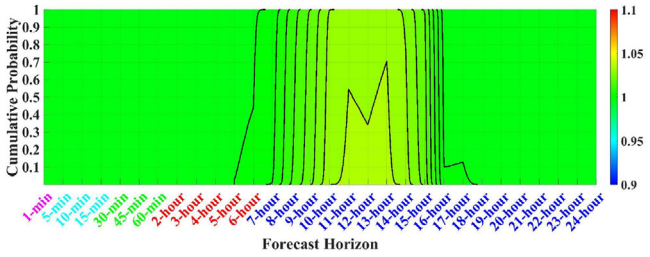

FIGURE 9 CP-based contour plot for visualisation of the congestion forecast at node 5, simulated with a constant-pf mode for Sorea's 7-bus system

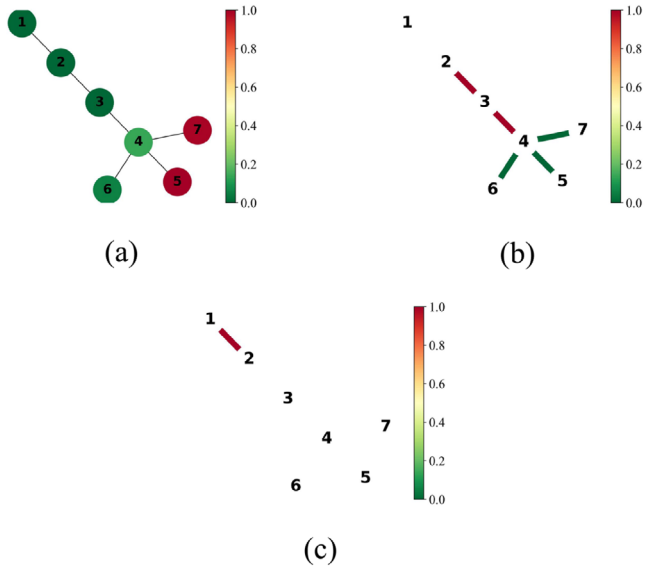

FIGURE 10 Colour-map visualising congestion forecast for 13-hour ahead simulated with a constant-pf mode for Sorea's 7-bus system. (a) Node voltages, (b) branches loading, (c) transformer loading

simulation uses the forecasted data for an entire day, starting from 00:00 hour. As the sun rises, the PV production increases, reaching its peak value around noon and decreasing after that. Thus, mainly the higher PV production level leads to an increase in the node voltages and vice-versa while the load has a negligible effect due to the small proportion.

5.1.2 | Colour-map

The colour-map is useful for evaluating the overall picture and the exact locations of the network congestion. The colourbar here represents the CP for congestion. For illustration purposes, the congestion threshold for the node voltage is taken as 1.03 p.u., for branches and transformer loading as 0.5 and 0.3 p.u., respectively. The DSO can specify its thresholds as desired.

It can be seen from Figure 10(a) that for a 13-hour ahead forecast, nodes 5 and 7 have high CP for voltage deviation; node 4 has medium CP while the rest nodes have low CP for voltage deviation. Similarly, Figure 10(b) shows that branches 2–3 and 3–4 have high CP for congestion, and the rest of the branches have low CP for congestion. Furthermore, Figure 10(c) shows

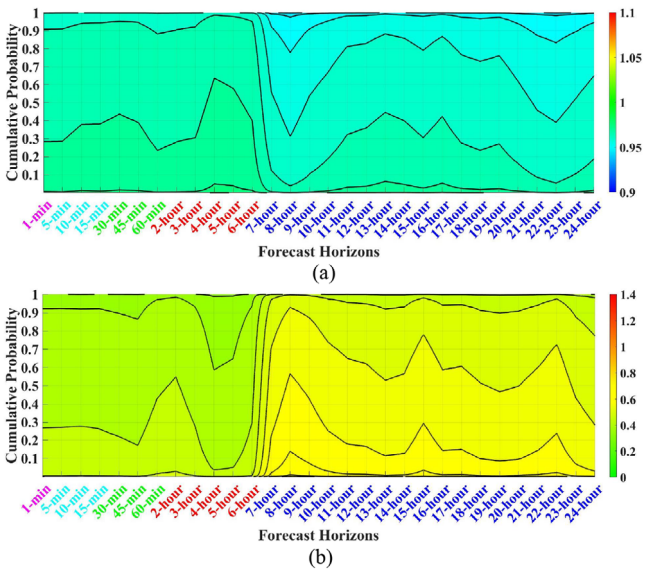

FIGURE 11 CP-based contour plots for visualisation of congestion forecast simulated with a constant-pf mode for the 141-bus distribution system with no PV production. (a) The voltage at node 141, (b) the loading level of branch 3–4

that the transformer has a high CP for overloading. Due to space limits, the colour-map for only one time horizon is presented here while the animated version of colour-map over different forecast horizons can be found at ref. [35].

5.2 | 141-bus distribution system of Caracas metropolitan area

5.2.1 | Visualisation of congestion forecast over a day

To visualise the congestion forecast over a day, the simulations are carried out with a constant-pf mode using the PV production and load forecasts profile, as shown in Figures 6 and 7, respectively. To illustrate the functionalities of the proposed tool, three different scenarios are considered, i.e. with no PV production, 50% of the PV production forecast, and 100% of the PV production forecast. With this tool, the node voltage and branches loading can be forecasted at all the system nodes and branches. Although, in this work, node 141 is chosen as it is one of the weakest nodes in terms of voltage variation, and branch 3–4 is chosen as it is one of the most loaded branches in the network.

- Scenario 1: No PV production
  This scenario can be treated as a base case, i.e. same as the original system without the consideration of any PV production. The CP-based contour plots for the voltage at node 141 and branch 3–4 are presented in Figure 11. It can be seen from Figure 11(a) that in the absence of any PV production, the node voltage remains below 1 p.u. as only the conventional loads are present in the system. It can also be observed

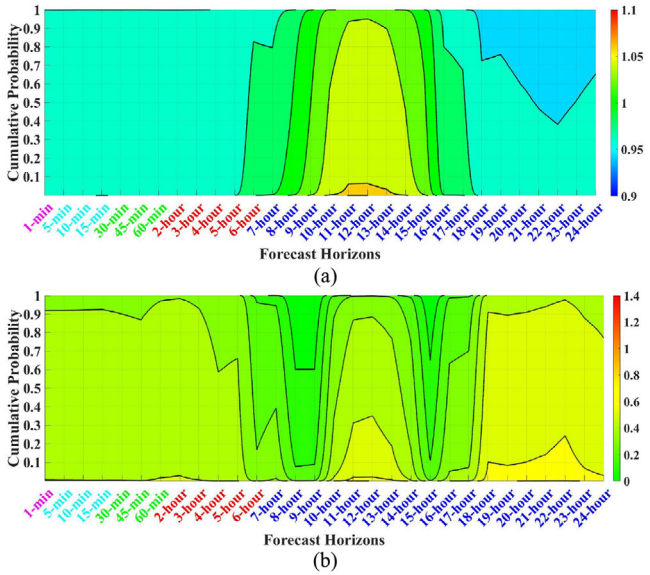

FIGURE 12 CP-based contour plots for visualisation of congestion forecast simulated with a constant-pf mode for the 141-bus distribution system considering the PV installations with 50% of the PV production forecast. (a) The voltage at node 141, (b) the loading level of branch 3–4

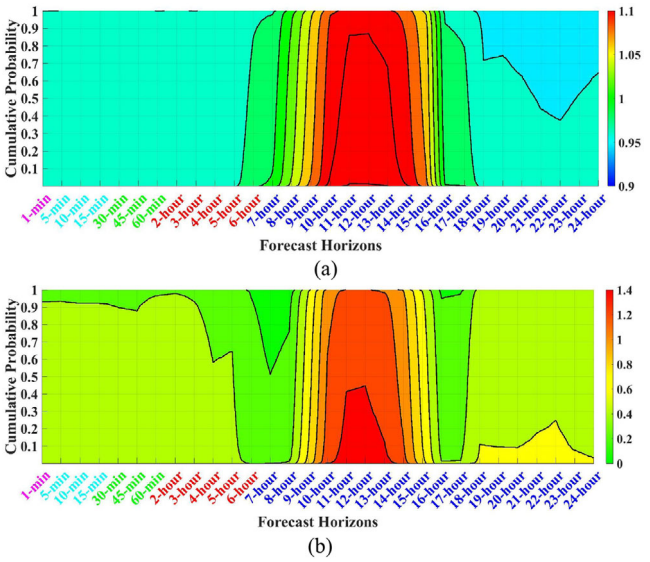

FIGURE 13 CP-based contour plots for visualisation of congestion forecast simulated with a constant-pf mode for the 141-bus distribution system considering PV installations with 100% of the PV production forecast. (a) The voltage at node 141, (b) the loading level of branch 3–4

that in the beginning (for initial forecast horizons) which are the mid-night hours, the contour plot remains green (close to 1 p.u.) and eventually starts turning towards blue as the morning hours approach and load starts increasing. Similarly, from Figure 11(b), it can be seen that the loading level of branch 3–4 largely remains around 50% during the initial forecast horizons and then increases to around 60% from 7-hour ahead until 22-hour ahead due to increased load demand during the day. Thus, it is clearly visible from CP-based contour plots (Figure 11) that the network is subjected to a different level of congestion over the considered forecast horizons. This scenario showcases the ability of the proposed tool in interactively forecasting the under and overvoltage problems in the network.

- Scenario 2: 50% of the PV production forecast
  In this scenario, the system has been modified to include PV installations at all the load buses. The same PV production profile (without affecting the generality of the results), as shown in Figure 6, is considered at all the load buses. Although the PV production at each bus is taken as 50% of the forecasted value and thus it varies between 0 to 204.5 kW. The CP-based contour plots for the voltage at node 141 and branch 3 − 4 are presented in Figure 12. It can be seen from Figure 12(a) that for 12-hour ahead, the CP for voltage to be above 1.05 p.u. at node 141 is approximately 0.95. Similarly, from Figure 12(b), for 12-hour ahead the CP for loading level of branch 3–4 to be above 0.5 p.u. is approximately 0.35. Figure 12(b) presents an interesting observation, that the loading level of branch 3–4 from 12-hour ahead until 17-hour ahead forecast horizons, is lesser as compared to the loading level obtained from the scenario without any PV production. This occurs because the PV production supplies the load locally which relieves congestion in the network or leads to reduced branch loading. Thus, the CP-based contour plots (Figure 12) show that the network is subjected to an assorting level of congestion over the considered forecast horizons mainly due to varying PV production and load demand during the day.
- Scenario 3: 100% of the PV production forecast
  In this scenario, the system has been modified to include PV installations at all the load buses. The same PV production profile (without affecting the generality of the results), as shown in Figure 6, is considered at all the PV nodes varying between 0 to 409.1 kW. The CP-based contour plots for the voltage at node 141 and branch 3–4 are presented in Figure 13. It can be seen from Figure 13(a) that for 12-hour ahead, the CP for voltage to be above 1.1 p.u. at node 141 is approximately 0.85. Similarly, from Figure 13(b), for both 11 and 12-hour. ahead the CP for loading level of branch 3–4 to be above 1 p.u. is approximately 1. Thus, it is clearly visible from CP-based contour plots (Figure 13) that the network is subjected to a different level of congestion over the considered forecast horizons. These changes in the congestion levels occur mainly due to varying PV production and load demand during the day.

5.2.2 | Impact of load models on congestion forecast results

To assess the impact of load models, four simulations with different load model parameters are carried out. The load model parameters for these simulations are presented in Table 3. The simulations consider the PV installations at all the load buses with the same PV production profile as shown in Figure 6, varying between 0 to 409.1 kW. The CP for voltage at node 141 and loading level of branch 3–4 for 13-hour ahead (maximum

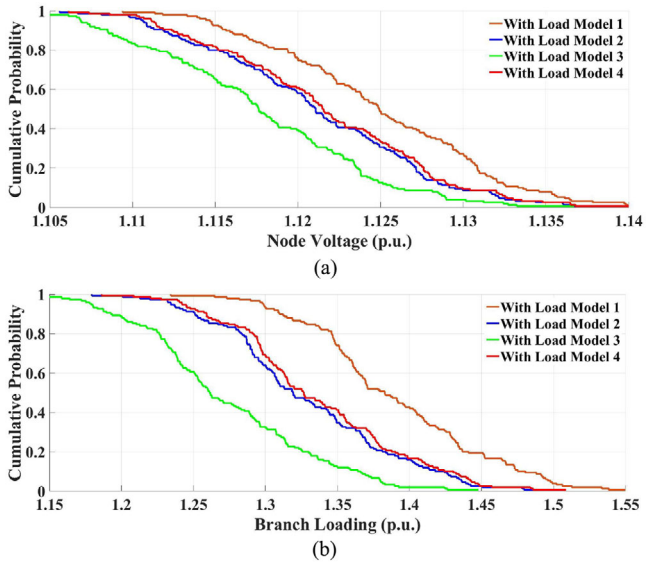

FIGURE 14 CP-based congestion indicators showing the impact of load models on congestion forecast for 13-hour ahead for the 141-bus distribution system. (a) The node voltage at node 141, (b) the loading level of branch 3–4

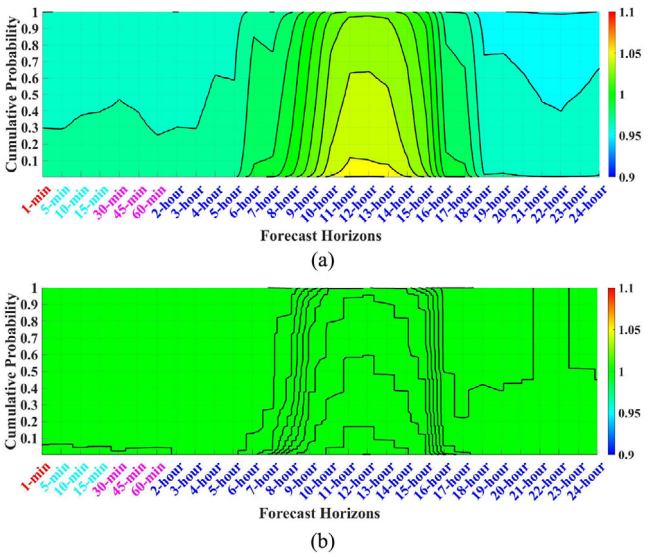

FIGURE 15 CP-based contour plots showing the influence of operating modes of PV-inverter on the congestion forecast for the 141-bus distribution system. (a) The voltage at node 141 with constant-pf mode, (b) the voltage at node 141 with constant-V mode

PV production) with different load models are shown in Figure 14(a,b), respectively.

It can be seen from Figure 14(a) that the node voltage deviation is highest with load model 1 (P). This can be explained using the "voltage drop" equation of a simple network. Assuming an increase in the PV production at a node, there will be an increase in the node voltage, and this change will not be affected by the constant power load (the consumed power will not change regardless of the change in voltage). While the node voltage deviation is lowest with load model 3 (Z) because the increase in PV production will lead to a rise in voltage initially. As the load is a constant-impedance load, the consumed power will increase with increased voltage, which leads to a higher line current and reduced node voltage. Hence, the node voltage deviation is lowest with load model 3 (Z) and highest with load model 1 (P). Further, with load models 2 and 3 (residential feeder and constant impedance), the node voltage is higher with the load model 2 because the voltage deviation will be higher in constant current load ($P \propto V$) than in constant impedance load ($P \propto V^2$), as the voltage is proportional to the power in I load while it is proportional to the square root of power in Z load. Similar explanations can be applied for branch loading with the different load models as shown in Figure 14(b). The results have shown that it is important to have good load models to have a more accurate congestion forecast, i.e. not over-or under-estimate the network's congestion levels.

5.2.3 | Influence of operating modes of PV-inverter on congestion forecast results

To assess the impact of operating modes of PV-inverter, the simulations are done with constant-pf and constant-V modes of operation. The simulations consider the PV installations at all

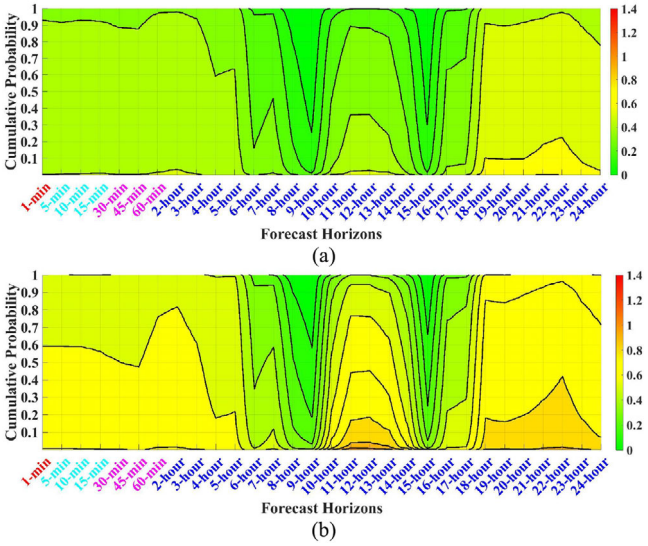

FIGURE 16 CP-based contour plots showing the influence of operating modes of PV-inverter on the congestion forecast for the 141-bus distribution system. (a) The loading level of branch 3–4 with constant-pf mode, (b) the loading level of branch 3–4 with constant-V mode

the load buses with the same PV production profile as shown in Figure 6, varying between 0 and 143.2 kW. The CP for voltage at node 141 and loading level of branch 3–4 under the two modes of operation are presented in Figures 15 and 16, respectively.

For 12-hour ahead, the CP for node voltage to be above 1.04 p.u. in constant-pf mode is 0.6 (Figure 15(a)) while in a constant-V mode it is 0 (Figure 15(b)). Similarly, for 12-hour ahead, the CP for branch loading to be above 0.8 p.u. in constant-V mode (Figure 16(b)) is approximately 0.2 while it is almost 0 in constant-pf mode (Figure 16(a)).

TABLE 5 Computational time for congestion forecast tool with different test systems (in seconds)

Sl. no.	Number of MCS	Sorea's 7-bus system		141-bus system	
		Tolerance limit		Tolerance limit	
		0.001 p.u.	0.00001 p.u.	0.001 p.u.	0.00001 p.u.
1	100	0.93	1.01	5.98	7.60
2	1000	3.89	4.50	58.34	75.04
3	10000	39.81	46.23	1239.13	1411.29

It is evident from the results that in a constant-V mode, the CP for nodes voltage has decreased but simultaneously the loading level of branches has increased. The reason for the reduced voltage deviation is due to the consideration of P-V nodes. In a constant-V mode, the voltage is maintained at a specified value through reactive power compensation by injection of higher reactive current, which leads to higher current and MVA loading in associated branches and transformers. Thus, the PV-inverter operating mode is an important aspect to be considered in the congestion forecast tool.

6 | SCALABILITY AND ACCURACY OF PROPOSED TOOL

The scalability of the proposed tool when applied to a large distribution system, is an important feature, which is considered during tool development. The tool is applied to a 7-bus feeder network of Sorea due to the availability of the physical solution for PV production and load forecasts. Further, the tool is applied to the 141-bus real distribution system to evaluate the scalability. The computational time (for all time horizons) for the two case studies in a constant-pf mode of operation is presented in Table 5. These results are obtained with MATLAB (R2019b version) and the computer configuration as Intel(R) Core(TM) i7-7700K CPU @4.20-GHz processor and 48 GB RAM.

The computational time of the algorithm depends on the number of MCS and the tolerance limit. The higher number of MCS and stricter tolerance limits would lead to a more accurate determination of the CP for congestion indicators which is the backbone for contour plots and colour-map. It can be seen from Table 5 that the computational time increases with the increase in the number of MCS and stricter tolerance limits. Thus, it is a trade-off situation between computational time and accuracy for the DSO. Like in the 141-bus system, with the given computer configuration, the most optimal solution appears as 1000 MCS and 0.001 p.u. tolerance limit.

Another important aspect is the accuracy of the congestion forecast, which mainly depends on the PV production and load forecasts accuracy. The lesser PV production and load forecasts error would lead to more accurate scenarios generation through MCS, and thus, the results of the congestion forecast will be more accurate. To validate this aspect, two congestion forecast simulations are performed with different forecast errors of PV production and load. The PV production and load forecasts errors used in these two simulations are shown in Table 4. For each congestion forecast, the mean and standard deviation for the normal distribution is calculated for node voltages and branch loading levels. The standard deviation for the voltage at node 141 and the loading level of branch 3–4, are presented in Figure 17(a,b).

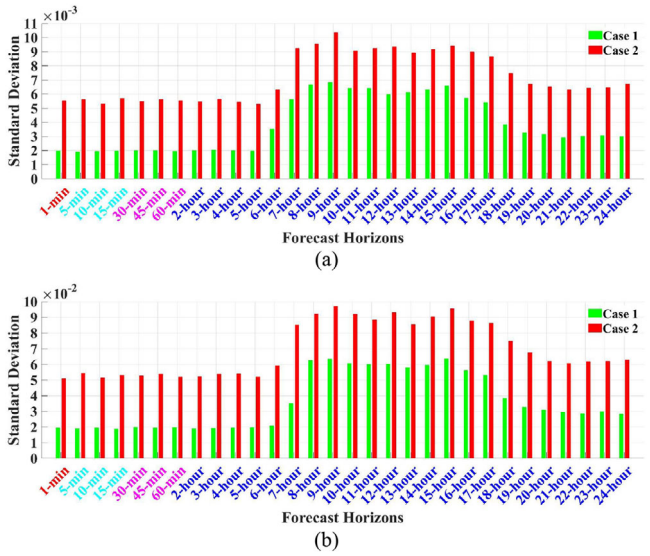

FIGURE 17 Standard deviation of congestion indicators simulated with different forecast errors for the 141-bus distribution system. (a) The node voltage at node 141, (b) the loading level of branch 3–4

It can be seen from Figure 17 that higher PV production and load forecasts errors lead to higher standard deviation of node voltages (Figure 17(a)) and branch loading (Figure 17(b)) as the forecast errors considered in Case 1 are lower as compared to Case 2. However, there is no substantial difference in the mean value of node voltages and branch loading in the two simulations as the same mean (μ) obtained from PV production and load forecasts is used in the Gaussian PDF for generating MCS in the two simulations.

7 | INTEGRATION AND DEMONSTRATION WITH EXISTING DISTRIBUTION MANAGEMENT SYSTEM

The integration and demonstration of the congestion forecast tool are done using the Codex Smart Edge solution of Atos

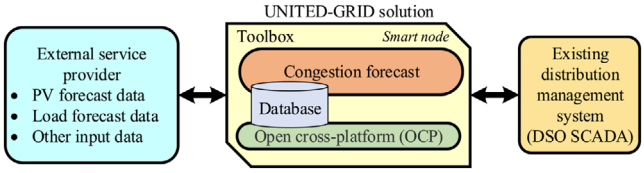

FIGURE 18 Functional diagram for tool integration and demonstration with the DSO SCADA

Worldgrid, which is an adaptable software solution used to set up an IoT and edge computing infrastructure [36]. The main motivations behind the integration and demonstration of the tool are validation on real test sites, compliance with the industrial standards, and reduced launch time to market. The integration and demonstration are performed for the 7-bus feeder of Sorea's distribution system in France as presented in Section 4.1. The solution which enables an integration of the congestion forecast tool is referred to as the UNITED-GRID solution (UGS). In this paper, UGS refers to only the congestion forecast tool while within the UNITED-GRID project it hosts several other tools as well. The functional diagram for the tool integration and demonstration with the existing DMS of the DSO is presented in Figure 18. The PV production and load forecasts solution as presented in Section 3.1 are also integrated with the UGS which provides inputs to the congestion forecast tool.

The description of the involved actors in the architecture of UGS is as follows.

- External service provider refers to the external data sources such as PV production forecast, load forecast, and other input data.
- Toolbox (TB) executes and supervises the implementation of the congestion forecast tool and the associated graphical interface along with the data management.
- Open cross-platform (OCP) collects and provides the data from/to the different actors. It also ensures the connectivity between the TB and external service providers, as well as the connectivity between the different instantiation of the UGS. The OCP also ensures data sharing and storing within the UGS.
- DSO SCADA platform refers to the existing SCADA system of the DSO.

The UGS dashboard login page for Sorea's demonstration site is shown in Figure 19. DSOs can connect through their account and get access to the UGS Dashboard.

The synoptic visualisation as presented in Figure 20 is based on the cumulative probability of the associated congestion indicators, i.e. nodes voltage or component's loading level. The colour code which has been assigned for the synoptic visualisation of the congestion indicators is presented in Table 6. Figure 20(a) represents an example of the synoptic visualisation for all the nodes voltage where all the nodes are shown in red colour which indicates that the CP_{node} for a threshold voltage level (chosen by the DSO) is greater than 0.9 (or 90% of the

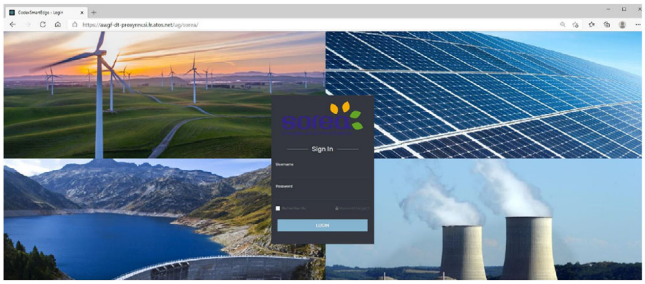

FIGURE 19 Dashboard login page for Sorea's demonstration site in France

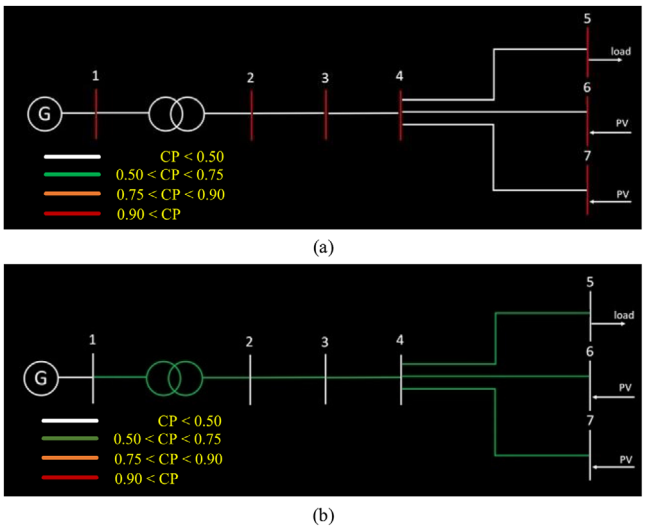

FIGURE 20 An example of synoptic visualisation for 7-bus feeder of Sorea's distribution system using the Codex Smart Edge platform. (a) Nodes voltage, (b) component's loading

times). Similar synoptic visualisation is presented in Figure 20(b) for branches and transformer. In the component visualisation, the threshold is selected in terms of percentage loading of the component, for instance, 60% or 80%.

The synoptic visualisation presents the implementation of the colourmap (presented in Section 5.1.2) within the UGS. The synoptic visualisation presents an overall picture of the network before the DSO. Once the system operator identifies the exact location of the congestion, then that specific node/component could be selected (in the synoptic visualisation) which will open the contour plot (presented in Section 5.1.1). Thus, the synoptic visualisation helps the operator to understand the

TABLE 6 Colour coding for the synoptic visualisation

Cumulative probability	Colour
$CP_{\text{node/component}} < 0.5$	White
$0.5 < CP_{\text{node/component}} < 0.75$	Green
$0.75 < CP_{\text{node/component}} < 0.9$	Orange
$CP_{\text{node/component}} > 0.9$	Red

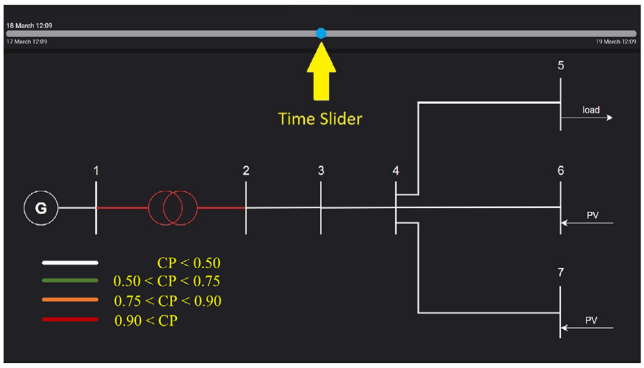

FIGURE 21 A snapshot of the synoptic visualisation for 7-bus feeder of Sorea's distribution system using the Codex Smart Edge platform

overall as well as component-specific network congestion picture. Further, the time slider empowers the system operator to select the desired forecast horizon for taking corresponding preventive action (discussed in Section 2.2.2).

Further, a snapshot of the synoptic visualisation of the congestion forecast tool for the 7-bus feeder of Sorea's distribution system is presented in Figure 21. It also shows a time slider through which the DSO can select a desired congestion forecast horizon (specific date and time). By moving the time slider, the synoptic is updated and then the operator can visualise the congestion forecast for the desired horizons (both historical and future). As can be seen from Figure 21, for the selected horizon, the transformer connected between $1-2$ is coloured as red which signifies that $CP_{\text{transformer}}$ must be greater than 0.9 for the threshold percentage loading which is set as 40% of transformer rated capacity. While the branches are coloured as white signifying that CP_{branch} of the branches must be less than 0.5 for the threshold percentage loading which is set as 80% of branch ampacity. It is important to highlight that these threshold limits are chosen such that network congestion can be visualised with the present limited amount of PV production at Sorea's site. However, the DSO can choose or vary these threshold limits according to their network conditions as mentioned in Section 2.

8 | CONCLUSION

This paper presents a tool to assist the DSO to forecast the congestion levels in their networks as per the preferences specified by the DSO. The tool is implemented using the probabilistic power flow model which employs the backward-forward sweep algorithm. The PV production forecast obtained by capturing the fast movement of clouds and load forecast obtained through an artificial neural network is provided as inputs to the congestion forecast tool. The tool can present the cumulative probability-based contour plots and colour-maps of the network which visualise the network loading conditions for the DSO and make it easy for the DSO to take necessary preventive or corrective actions. The tool has also incorporated various important factors such as PV production and load forecasts accuracy, load models, and PV-inverter operating modes, which can impact the accuracy of network congestion and their simulation results are presented in the paper. The scalability of the proposed tool is studied by applying it to a large size distribution system. The tool performs satisfactorily in forecasting network congestion for various time-horizons with acceptable calculation time and accuracy for a relatively large network. The tool has been integrated via an IoT platform Codex Smart Edge of Atos Worldgrid to be ready for market exploitation for real-world applications. The tool will be used by the DSOs to support their daily congestion management tasks and better utilise their grids and thus reduce the need for expensive network reinforcement. The electricity consumers will also be benefitted from the tool as the distribution network will be operated more securely and eventually incur lesser network congestion costs.

ACKNOWLEDGMENTS

The work presented in this paper is financially supported by the following projects: (i) UNITED-GRID - received funding from the European Community's Horizon 2020 Framework Programme under grant agreement no. 773717; (ii) FLEXI-GRID - received funding from the European Community's Horizon 2020 Framework Programme under grant agreement no. 864048.

ORCID

Ankur Srivastava https://orcid.org/0000-0003-0362-7311

REFERENCES

1. European Commission. A European Green Deal. https://ec.europa.eu/info/strategy/priorities-2019-2024/european-green-deal_en, accessed 27 May 2021 (2019).
2. IRENA, European Commission. Renewable energy prospects for the European Union. https://www.irena.org/publications/2018/Feb/Renewable-energy-prospects-for-the-EU, accessed 27 May 2021 (2018).
3. Fairley, P.: Hawaii's solar push strains the grid. MIT Technology Review. https://www.technologyreview.com/s/534266/hawaiis-solar-push-strains-the-grid/, accessed 27 May 2021 (2015).
4. Prah, P. M. : Utility companies have a solar power problem. Governing USA. https://www.governing.com/news/headlines/utility-companies-have-a-.html, accessed 27 May 2021 (2014).
5. Liz Hobday. Electricity distributors warn excess solar power in network could cause blackouts, damage infrastructure. Australian Broadcasting Corporation. https://www.abc.net.au/news/2018-10-11/electricity-distributors-warn-excess-solar-could-damage-grid/10365622, accessed 27 May 2021 (2018).
6. Schermeyer, H., et al.: Understanding distribution grid congestion caused by electricity generation from renewables. In: Smart Energy Research. At the Crossroads of Engineering, Economics, and Computer Science, pp. 78–89. Springer, Berlin, Heidelberg (2017)
7. Nair, U.R., et al.: Grid congestion mitigation and battery degradation minimisation using model predictive control in PV-based microgrid. IEEE Trans. Energy Convers. 36(2), 1500–1509 (2020)
8. Widén, J., et al.: Probabilistic load flow for power grids with high PV penetrations using copula-based modeling of spatially correlated solar irradiance. IEEE J. Photovoltaics 7(6), 1740–1745 (2017)
9. Reddy, S.S.: Optimal scheduling of thermal-wind-solar power system with storage. Renewable Energy 101, 1357–1368 (2017)
10. Reddy, S.S., Momoh, J.A.: Realistic and transparent optimum scheduling strategy for hybrid power system IEEE Trans. Smart Grid 6(6), 3114–3125 (2015)

11. Hartvigsson, E., et al.: Estimating national and local low-voltage grid capacity for residential solar photovoltaic in Sweden, UK and Germany. Renewable Energy 171, 915–926 (2021)
12. Huang, S., Wu, Q.: Real-time congestion management in distribution networks by flexible demand swap. IEEE Trans. Smart Grid 9(5), 4346–4355 (2017)
13. Prettico, G., et al.: Distribution system operators observatory 2018. Publications Office of the European Union, Luxembourg (2019)
14. Huang, S., et al.: Distributed optimization-based dynamic tariff for congestion management in distribution networks. IEEE Trans. Smart Grid 10(1), 184–192 (2017)
15. Reddy, S.S.: Multi-objective based congestion management using generation rescheduling and load shedding. IEEE Trans. Power Syst. 32(2), 852–863 (2016)
16. Masaud, T.M., et al.: Placement of large-scale utility-owned wind distributed generation based on probabilistic forecasting of line congestion. IET Renewable Power Gener. 11(7), 979–986 (2017)
17. Srivastava, A. et al.: A congestion forecast framework for distribution systems with high penetration of PVs and PEVs. In: 2019 IEEE PES PowerTech Conf., pp. 1–6. IEEE (2019)
18. Fan, M. & Huang, L. : Probabilistic power reserve evaluation algorithm for power systems considering high solar energy penetration. In: IEEE Power and Energy Society General Meeting, pp. 1–5. IEEE (2018)
19. Abad, M.S.S., et al.: Probabilistic assessment of hosting capacity in radial distribution systems. IEEE Trans. Sustainable Energy 9(4), 1935–1947 (2018)
20. Nijhuis, M., Gibescu, M., Cobben, S.: Gaussian mixture based probabilistic load flow for LV-network planning. IEEE Trans. Power Syst. 32(4), 2878–2886 (2018)
21. Lujano.Rojas, J.M., et al.: Probabilistic methodology for estimating the optimal photovoltaic capacity in distribution systems to avoid power flow reversals. IET Renewable Power Gener. 12(9), 1045–1064 (2018)
22. Flores, G.C., et al.: Data-driven probabilistic power flow analysis for a distribution system with renewable energy sources using Monte Carlo simulation. IEEE Trans. Ind. Appl. 55(1), 174–181 (2018)
23. Hitachi ABB Power Grids. Network Manager ADMS. https://www.hitachiabb-powergrids.com/offering/product-and-system/scada/network-management/network-manager-adms, accessed 27 May 2021 (2020).
24. Siemens. Spectrum Power ADMS. https://new.siemens.com/global/en/products/energy/energy-automation-and-smart-grid/grid-control/advanced-distribution-management.html, accessed 27 May 2021 (2021).
25. Schneider Electric. "EcoStruxure™". Available at https://www.se.com/ww/en/work/solutions/for-business/electric-utilities/advanced-distribution-management-system-adms/, accessed 27 May 2021 (2021).
26. Zhang, C., et al.: FLECH: A Danish market solution for DSO congestion management through DER flexibility services. J. Modern Power Syst. Clean Energy 2(2), 126–133 (2014)
27. SORÉA. https://www.sorea-maurienne.fr/, accessed 27 May 2021 (2021).
28. IEEE Task Force on Load Representation for Dynamic Performance: Bibliography on load models for power flow and dynamic performance simulation. IEEE Trans. Power Syst. 10(1), 523–538 (1995)
29. Haque, M.: Load flow solution of distribution systems with voltage dependent load models. Electr. Power Syst. Res. 36(3), 151–156 (1996)
30. IEEE standard for interconnection and interoperability of distributed energy resources with associated electric power systems interfaces. In: IEEE Standard 1547-2018, pp. 1–227. IEEE (2018)
31. Cheng, C.S., Shirmohammadi, D.: A three-phase power flow method for real-time distribution system analysis. IEEE Trans. Power Syst. 10(2), 671–679 (1995)
32. UNITED.GRID. https://united-grid.eu/, accessed 27 May 2021 (2021).
33. Khodr, H., et al.: Maximum savings approach for location and sizing of capacitors in distribution systems. Electr. Power Syst. Res. 78(7), 1192–1203 (2008)
34. Balram, P., Tuan, L.A. & Carlson, O. : Predictive voltage control of batteries and tap changers in distribution system with photovoltaics. In: IEEE Power Systems Computation Conf., pp. 1–7. IEEE (2016)
35. Animated Colourmap Indicators. Available at http://publications.lib.chalmers.se/img/srivastava/, accessed 27 May 2021 (2021).
36. ATOS. https://atos.net/en/, accessed 27 May 2021 (2021).

How to cite this article: Srivastava, A., et al.: Development of a DSO support tool for congestion forecast. IET Gener. Transm. Distrib. 1–15 (2021). https://doi.org/10.1049/gtd2.12266

APPENDIX

The branches and transformer data for the part of Sorea's system are presented in Table A.1. The branches have different lengths with the same per unit-length parameters. The branches' ampacity and the transformer rating are also given.

TABLE A.1 Branches and transformer parameters for Sorea's grid

Sl. No.	Location	Resistance ($m\Omega$)	Reactance ($m\Omega$)	Susceptance (μS)	Capacity (kVA/Amp)
Transformer (LV-side)					
1	1–2	3.0637	14.9269	-	250
Branches					
2	2–3	9.4350	13.2418	0.1319	350
3	3–4	21.6376	30.3679	0.3026	350
4	4–5	23.2679	5.0894	0.1847	350
5	4–6	27.2495	4.4271	0	350
6	4–7	7.5420	4.1469	0.1150	350